Advances in Materials
2020; 9(2): 15-27
http://www.sciencepublishinggroup.com/j/am
doi: 10.11648/j.am.20200902.11
ISSN: 2327-2503 (Print); ISSN: 2327-252X (Online)

Review Article

Magnetoelectric Composites: Modeling and Application

Mirza Bichurin*, Roman Petrov, Alexander Tatarenko

Institute of Electronic and Information System, Novgorod State University, Veliky Novgorod, Russia

Email address:
Mirza.Bichurin@novsu.ru (M. Bichurin)
*Corresponding author

To cite this article:
Mirza Bichurin, Roman Petrov, Alexander Tatarenko. Magnetoelectric Composites: Modeling and Application. *Advances in Materials*. Vol. 9, No. 2, 2020, pp. 15-27. doi: 10.11648/j.am.20200902.11

Received: February 27, 2020; **Accepted**: March 12, 2020; **Published**: April 28, 2020

Abstract: The progress in electronic technology is directly coupled with the advances made in materials science. Within the broad class of materials available today, functional materials provide unique opportunity for developing novel components and devices as their physical and chemical properties. A combination of ferromagnetic and ferroelectric materials provides a new class of functional materials, termed as magnetoelectrics. An overview of modern magnetoelectric composites and examples of the design of electronic devices based on them are presented. The feature of these materials is that their parameters changes under the influence of an external magnetic and electric fields. The behavior of magnetoelectric composites in the wide frequency range is considered. Modeling of ME composites at low frequencies and in the field of electromechanical, ferromagnetic and magnetoacoustic resonances has shown that they can be effectively used to design various electronic devices in a wide frequency range. Nomographs method which can be used to plot the ME parameters versus initial material parameters and component volume fractions is presented. Nomographs can be used for a quick test of ME composites for applications where an approximate answer is appropriate and useful. Examples of ME composites application such as: magnetic field sensors, current sensors, microwave phase shifters, filters, attenuators, isolators are presented.

Keywords: Magnetoelectric Composites, Modeling, Application, Electronic Devices

1. Introduction

The review is devoted to the study and application of magnetoelectric (ME) composites based on magnetic-piezoelectric layered structures in electronic devices [1-3]. Historically, to the use of ME composites for practical purposes, the researchers came after numerous studies of single-crystal magnetoelectrics, which showed that ME interactions in most of them are observed at temperatures well below room temperature and the ME coefficients vanish once the temperature approaches the transition point to an unordered state, which is due to the low temperatures of Neel or Curie for these materials. In addition, single-crystal magnetoelectrics are characterized by small values of ME coefficients, the magnitude of which is insufficient for practical applications. To a great extent, the bulk and layered ME composites are free from these shortcomings. For such ME composites, there are wide possibilities for varying their physical properties, and thus optimizing the characteristics of devices based on them. The mechanism of ME interactions in composites can be considered as a result of the interaction of piezoelectric and magnetostrictive properties, which consists in the following: an external electric field causes deformation of the piezoelectric component, which leads to the appearance of mechanical stresses in the magnetostrictive component. The magnetostrictive component is magnetized due to the magnetostriction and a change in the magnetic properties, as a result, occurs in the external electric field. It should be noted that the opposite effect is possible: applying an external magnetic field will lead to a change in the electrical properties of the composite. In practice, we are talking about pseudo-piezomagnetism, when the magnetostrictive properties of ferrite are used in the application of an additional variable magnetic field of small amplitude. Comparison of bulk and layered ME composites shows a significant advantage of the latter in terms of the ME coefficients attained, which is due to the low electrical resistance of the ferrite phase. Therefore, all modern investigations in the wide frequency

range are carried out on layered ME composite composites: single-crystal ferrite and piezoelectric layers. In this case, the layers can be made both in the form of separate plates, and in the form of films on substrates. Physics and technology of magnetoelectric phenomena are considered in this review.

2. Low Frequency Magnetoelectric Effect

The theoretical modeling of low-frequency ME effect in layered and bulk composites based on magnetostrictive and piezoelectric materials rests on the effective-medium approach and exact calculation based on elastostatic, electrostatic and magnetostatic equations. The expressions for effective parameters including ME susceptibilities and ME voltage coefficients as functions of material parameters and volume fractions of components are obtained. Longitudinal, transverse and in-plane field orientations are considered. The use of the offered model has allowed to estimate the ME effect in ferrite cobalt - barium titanate, ferrite cobalt - PZT, ferrite nickel - PZT, lanthanum-strontium manganite - PZT composites adequately. Using layered structures enables one to overcome a series of difficulties that are characteristic for bulk composites. The reasons for the giant ME effects in layered composites are: (a) high piezoelectric and piezomagnetic coefficients in individual layers, (b) effective stress transfer between layers, (c) ease of poling and subsequent achievement of a full piezoelectric effect, and (d) ability to hold charge due to suppression of leakage currents across composites with a 2-2 connectivity.

Our approach is based on continuum mechanics, and considers the composite as a homogeneous medium having piezoelectric and magnetostrictive subsystems. To derive the effective material parameters of composites, an averaging method consisting of two steps [4-8] should be used. In the first step, the composite is considered as a structure whose magnetostrictive and piezoelectric phases are distinct and separable. ME composites are characterized by the presence of magnetic and electric subsystems interacting with each other.

The constitutive equation for the piezoelectric effect can be given in the following form:

$$ {}^{p}S_i = {}^{p}s_{ij}\,{}^{p}T_j + {}^{p}d_{ki}\,{}^{p}E_k, \tag{1} $$

$$ {}^{p}D_k = {}^{p}d_{ki}\,{}^{p}T_i + {}^{p}\varepsilon_{kn}\,{}^{p}E_n; \tag{2} $$

where ${}^{p}S_i$ is astrain tensor component of the piezoelectric phase; ${}^{p}E_k$ is a vector component of the electric field; ${}^{p}D_k$is a vector component of the electric displacement; ${}^{p}T_i$ is astress tensor component of the piezoelectric phase; ${}^{p}s_{ij}$is a compliance coefficient of the piezoelectric phase; ${}^{p}d_{ki}$ is a piezoelectric coefficient of the piezoelectric phase; and ${}^{p}\varepsilon_{kn}$ is a permittivity matrix of the piezoelectric phase.

Analogously, the strain and magnetic induction tensors of the magnetostrictive phase are respectively:

$$ {}^{m}S_i = {}^{m}s_{ij}\,{}^{m}T_j + {}^{m}q_{ki}\,{}^{m}H_k \tag{3} $$

$$ {}^{m}B_k = {}^{m}q_{ki}\,{}^{m}T_i + {}^{m}\mu_{kn}\,{}^{m}H_n, \tag{4} $$

where ${}^{m}S_i$ is a strain tensor component of the magnetostrictive phase; ${}^{m}T_j$ is a stress tensor component of the magnetostrictive phase; ${}^{m}s_{ij}$ is a compliance coefficient of the magnetostrictive phase; ${}^{m}H_k$ is a vector component of magnetic field; ${}^{m}B_k$ is a vector component of magnetic induction; ${}^{m}q_{ki}$ is a piezomagnetic coefficient; and ${}^{m}\mu_{kn}$ is a permeability matrix.

In the second step of the averaging method to derive the effective materials parameters, the bilayer composite is considered as a homogeneous solid, whose behavior can be described by the following coupled sets of linear algebraic equations:

$$ \begin{aligned} S_i &= s_{ij}T_j + d_{ki}E_k + q_{ki}H_k, \\ D_k &= d_{ki}T_i + \varepsilon_{kn}E_n + \alpha_{kn}H_n, \\ B_k &= q_{ki}T_i + \alpha_{kn}E_n + \mu_{kn}H_n; \end{aligned} \tag{5} $$

where S_i *is a* strain tensor component; T_j is a stress tensor component; E_k *is a* vector component of the electric field; D_k *is a* vector component of the electric displacement; H_k *is a* vector component of the magnetic field; B_k *is a* vector component of the magnetic induction; $s_{ij}$is an effective compliance coefficient; d_{ki} *is a* piezoelectric coefficient; q_{ki} *is a* piezomagnetic coefficient; ε_{kn} is an effective permittivity; $\mu_{kn}$is a permeability coefficient; and α_{kn} *is a* ME coefficient.

The simultaneous solution of the coupled sets of linear algebraic equations allows one to find the effective parameters of a composite. Using boundary conditions for magnetic and electric fields, and using open circuit condition, one can then obtain the following expressions for longitudinal (Figure 1) ME voltage coefficient:

$$ \alpha_{E,33} = \frac{E_3}{H_3} = 2\frac{\mu_0 v(1-v)\,{}^{p}d_{31}\,{}^{m}q_{31}}{\{2\,{}^{p}d_{31}^2(1-v) + {}^{p}\varepsilon_{33}[({}^{p}s_{11}+{}^{p}s_{12})(v-1) - v({}^{m}s_{11}+{}^{m}s_{12})]\}} \times \frac{[({}^{p}s_{11}+{}^{p}s_{12})(v-1) - v({}^{m}s_{11}+{}^{m}s_{12})]}{\{[\mu_0(v-1) - {}^{m}\mu_{33}v][v({}^{m}s_{12}+{}^{m}s_{11}) - ({}^{p}s_{11}+{}^{p}s_{12})(v-1)] + 2\,{}^{m}q_{31}^2 v^2\}} \times \tag{6} $$

Figure 1. *Schematic of the layered composite structure for longitudinal case.*

Next we consider the transverse fields' orientation. The expressions for transverse (Figure 2) ME voltage coefficient:

$$ \alpha_{E,31} = \frac{E_3}{H_1} = \frac{-v(1-v)({}^{m}q_{11}+{}^{m}q_{21})\,{}^{p}d_{31}}{{}^{p}\varepsilon_{33}({}^{m}s_{12}+{}^{m}s_{11})v + {}^{p}\varepsilon_{33}({}^{p}s_{11}+{}^{p}s_{12})(1-v) - 2\,{}^{p}d_{31}^2(1-v)} \tag{7} $$

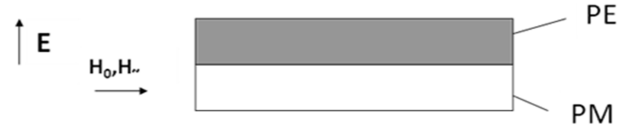

Figure 2. *Schematic of the layered composite structure for transverse case.*

In Figure 3 the experimental results for both cases for ME

bilayer structures are presented: 15 NFO layers and 14 PZT layers, at room temperature and 100 Hz.

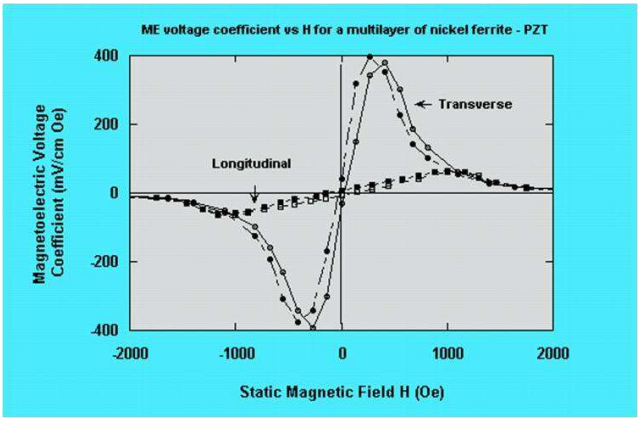

Figure 3. *ME voltage coefficients for NFO/PZT structures.*

Transverse ME voltage coefficient is larger than the longitudinal one, this is due fact that ME voltage coefficients proportional to product of d_{31} and q_{11}, or q_{31}, and q_{11} is more larger then q_{31}.

3. Magnetoelectric Effect at Resonance Area

To create new magnetoelectric composites with enhanced ME couplings we discuss the ME properties of magnetostrictive-piezoelectric composites. Such materials would enable one to make novel functional electronics devices. The main objective is a comparative analysis of ME composites that have different connectivity types. It is to emphasize that multilayer composites possess giant ME responses and at the same time the relative simplicity of manufacturing. The ultimate purpose of theoretical estimates is to predict the ME susceptibility and ME voltage coefficients as the most basic parameters of magnetoelectricity. The magnetoelectric effects occur over a broad frequency bandwidth, extending from the static to millimeter ranges.

3.1. Magnetoelectric Effect in the EMR Range

The magnetoelectric (ME) effect in composites is caused by mechanically coupled magnetostrictive and piezoelectric subsystems: it is present in neither subsystem separately. Under magnetic field owing to the magnetostriction of the magnetic component, there are stresses which are elastically transmitted in the piezoelectric phase resulting in polarization changes via piezoelectricity. Because the ME effect in composites is due to mechanically coupled piezoelectric and magnetostrictive subsystems, it sharply increases in the vicinity of the electromechanical resonance (EMR) frequency [16-20].

The theoretical model is based on the exact solution of the equations of motion of the medium and uses the material parameters of the original components of the structure.

The equations of motion of the medium for Longitudinal mode:

$$\rho \frac{\partial^2 u_i}{\partial t^2} = V \frac{\partial {}^{p}T_{ij}}{\partial x_j} + (1-V)\frac{\partial {}^{m}T_{ij}}{\partial x_j} \tag{8}$$

where $i, j = 1, 2, 3$ is axes indexes (x_1— axe x, x_2—axe y, x_3— axe z), u_i is composite displacement along the axis x_i, $\bar{\rho} = V^{p}\rho + (1-V)^{m}\rho$ is average density of composite, V is volume fraction of a piezoelectric, ${}^{p}\rho$, ${}^{m}\rho$, ${}^{p}T_{ij}$ и ${}^{m}T_{ij}$ is densities and components of the stress tensor of the piezoelectric and ferromagnetic components, respectively. Simultaneous solution of elasticity equations and Eq. 8 by use of appropriate boundary conditions allows one to find the ME voltage coefficient. Since the solution depends on the composite shape and orientation of applied electric and magnetic fields, we consider some of the most general cases. In Figure 4 presented thin layered magnetostrictive-piezoelectric rectangular plate.

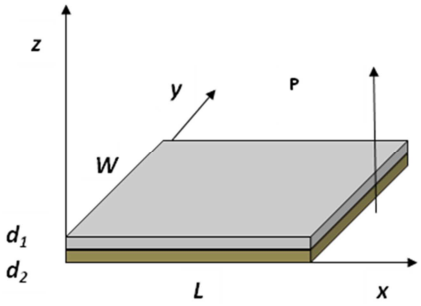

Figure 4. *Thin layered magnetostrictive-piezoelectric rectangular plate. The direction of polarization is indicated by an arrow.*

Expressions for the components of the magnetic layer deformation ${}^{m}S_i$, piezoelectric layer ${}^{p}S_i$ and electric displacement ${}^{p}D_3$ of piezoelectric layer in the case when a bias field directed perpendicular to the plate (along the z axis):

$$\begin{aligned}
{}^{p}S_1 &= {}^{p}s_{11}{}^{p}T_1 + {}^{p}s_{12}{}^{p}T_2 + {}^{p}d_{31}E_3,\\
{}^{p}S_2 &= {}^{p}s_{12}{}^{p}T_1 + {}^{p}s_{11}{}^{p}T_2 + {}^{p}d_{31}E_3,\\
{}^{m}S_1 &= {}^{m}s_{11}{}^{m}T_1 + {}^{m}s_{12}{}^{m}T_2 + {}^{m}q_{31}H_3,\\
{}^{m}S_2 &= {}^{m}s_{12}{}^{m}T_1 + {}^{m}s_{11}{}^{m}T_2 + {}^{m}q_{31}H_3,\\
{}^{p}D_3 &= {}^{p}\varepsilon_{33}E_3 + {}^{p}d_{31}\,({}^{p}T_1 + {}^{p}T_2),
\end{aligned} \tag{9}$$

where ${}^{p}T_i$ is the stress and ${}^{p}s_{ii}$ is the compliance of the ferroelectric at constant electric field, ${}^{m}T_i$ is the stress and ${}^{m}s_{ii}$ is the compliance of the ferromagnetic at constant magnetic field, ${}^{p}\varepsilon_{33}$ is the relevant component of the electrical permittivity, ${}^{p}d_{31}$ is the piezoelectric coefficient of the ferroelectric, ${}^{m}q_{ij}$ is the piezomagnetic coefficient of ferromagnetic, E_3 and H_3 are ac electric and magnetic fields. Close to EMR we can assume ${}^{m}T_1 >> {}^{m}T_2$ and ${}^{p}T_1 >> {}^{p}T_2$ (axis 1 is directed along the plate length) such that ${}^{m}T_2$ and ${}^{p}T_2$ may be ignored.

The expression for the longitudinal ME voltage coefficient:

$$\alpha_{E,33} = \frac{2{}^{p}d_{31}{}^{m}q_{31}{}^{p}s_{11}V(1-V)\tan(kL/2)}{s_1\left({}^{p}d_{31}^2 - {}^{p}s_{11}{}^{p}\varepsilon_{33}\right)kL - 2{}^{p}d_{31}^2V{}^{m}s_{11}\tan(kL/2)} \tag{10}$$

where $s_1 = V^m s_{11} + (1 - V)^p s_{11}$.

The expression for the transverse ME voltage coefficient:

$$\alpha_{E,31} = \frac{2^p d_{31}\, {}^m g_{11} \mu_{eff}\, {}^p s_{11} V(1-V)\tan(kL/2)}{s_{21}\left({}^p d_{31}^2 - {}^p s_{11}\, {}^p \varepsilon_{33}\right) kL - 2\, {}^p d_{31}^2 V\, {}^m s_{11} \tan(kL/2)} \quad (11)$$

where $s_2 = V^m s^B_{11} + (1 - V)^p s_{11}$.

The value of the ME voltage coefficients is directly proportional to the product of the piezoelectric d_{31} and the piezomagnetic modules q_{31} or g_{11}. In real structures, there are losses that must be taken into account in the calculations.

In Figure 5 and 6 presented a comparison of calculation and experimental data. The calculated data are represented by a solid line, experimental are dots.

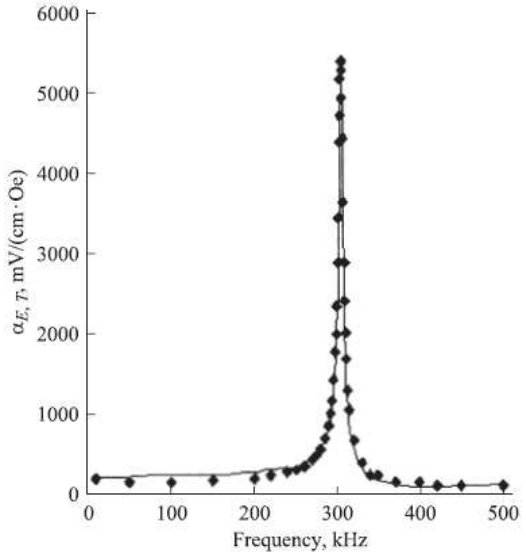

Figure 5. *The frequency dependence of the transverse ME voltage coefficient for a two-layer the nickel ferrite -PZT structure.*

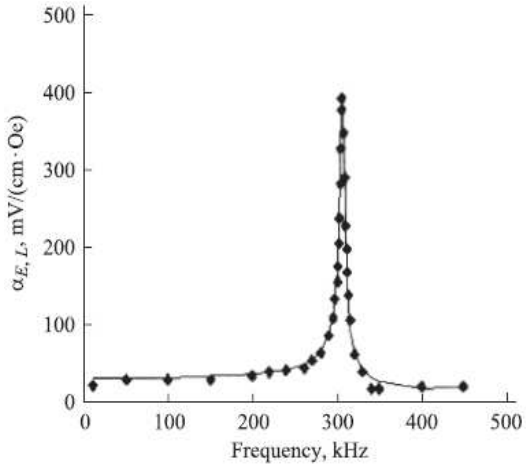

Figure 6. *The frequency dependence of the longitudinal ME voltage coefficient for a two-layer the nickel ferrite -PZT structure.*

Material parameters of the initial components:

Nickel ferrite: ${}^m s_{11}=6.5\cdot10^{-12}$ m^2/N, ${}^m s_{12}=-2.4\cdot10^{-12}$ m^2/N, ${}^m q_{31}=70\cdot10^{-12}$ m/A, ${}^m q_{11}=-680\cdot10^{-12}$ m/A, ${}^m q_{12}=125\ 10^{-12}$ m/A, ${}^m\varepsilon_{33}/\varepsilon_0=10$;

PZT: ${}^p s_{11}=15.3\cdot10^{-12}$ m^2/N, ${}^p s_{12}=-5\cdot10^{-12}$ m^2/N, ${}^p d_{31}=-175\cdot10^{-12}$ m/V, ${}^p\varepsilon_{33}/\varepsilon_0=1750$.

The loss parameter was empirically determined from the width of the EMR line. As seen, data and calculation results are in good agreement.

3.2. Magnetoelectric Effect in the FMR Range

ME composites offer important applications in the microwave range [21, 23]. In this frequency range, the ME effect reveals itself as a change in the magnetic susceptibility under an external electric field. Investigations of a ferromagnetic resonance (FMR) line shift by an applied electric field are easily performed for layered ferrite–piezoelectric structures. In addition, layered composites are of interest for applications as electrically tunable microwave phase shifters, devices based on FMR, magnetic-controlled electrooptical and/or piezoelectric devices, and electrically readable magnetic (ME) memories [1, 21, 23].

The phenomenological theory describing this effect is based on the fact that the magnetic susceptibility is a function of deformation, and that this dependence is determined by the piezoelectric and magnetoelastic constants of the piezoelectric and magnetostrictive phases, respectively.

The model of a bilayer structure, consisting of a ferrite spinel with cubic (m3 m) symmetry and poled lead zirconate titanate (PZT) with symmetry of ∞ m is considered. The influence of an electric field on the piezoelectric PZT phase can be described as follows:

$$ {}^pT_{ij} = {}^p c_{ijkl}\, {}^pS_{kl} - e_{kij}E_k \quad (12)$$

where E_k is a component of the electric field vector; and ${}^pT_{ij}$, ${}^pS_{kl}$, e_{kij}, ${}^pc_{ijk}$ are the components of the stress, strain, piezoelectric, and elastic stiffness tensors of the piezoelectric phase, respectively.

In the case when the electric field is applied along the polarization axis, i.e. $E_3 = E$, $E_1 = E_2 = 0$, it is:

$$\begin{aligned} {}^pT_{33} &= -e_{33}E + {}^p c_{13}({}^pS_{11} + {}^pS_{22}) + {}^p c_{33}{}^pS_{33}, \\ {}^pT_{11} &= -e_{31}E + {}^p c_{11}{}^pS_{11} + {}^p c_{12}{}^pS_{22} + {}^p c_{13}{}^pS_{33}=0, \\ {}^pT_{22} &= -e_{31}E + {}^p c_{12}{}^pS_{11} + {}^p c_{11}{}^pS_{22} + {}^p c_{13}{}^pS_{33}=0. \end{aligned} \quad (13)$$

Here ${}^mT_{ij}$ и ${}^mS_{kl}$ are tensors of stresses and deformations of the magnetostrictive phase, respectively.

To calculate the ME effect of bilayer structures in the FMR range, we should use the following procedure: (i) ${}^mS_3$ is defined as a function of the stress ${}^mT_3$; (ii) ${}^pT_3$ is defined as a function of the strain ${}^pS_3$; and (iii) use the known expressions for the dependence of the resonant magnetic field on stress to determine the FMR line shift. Thus, the task is reduced to the solutions of electrostatic equations under specific boundary conditions. Let us then consider that the bilayer structure is mechanically clamped along the 3 axis the ferrite and piezoelectric subsystems. In this case, the boundary conditions, without taking into account forces of friction, have the form:

$$ {}^pT_3 = {}^mT_3,\ {}^pS_3 = -\,{}^mv/{}^pv \cdot {}^mS_3,$$

where ^{m}v $u^{p}v$ arevolume fractions of the magnetostrictive and piezoelectric phases, respectively. Then we get:

$$^{m}T_3 = \frac{E_3\left(\frac{2^{p}c_{13}e_{31}}{^{p}c_{11}+^{p}c_{12}} - e_{33}\right)}{1+\frac{^{m}v}{^{p}v}\left(\frac{1}{3^{m}c_{44}}+\frac{1}{3\left(^{m}c_{11}+2^{m}c_{12}\right)}\right)\left(^{p}c_{33}-2\frac{^{p}c_{13}^2}{\left(^{p}c_{11}+^{p}c_{12}\right)}\right)} \quad (14)$$

It is known that applying a voltage leads to a change in the resonant magnetic field. In case when both the magnetic and electric fields are oriented along the polarization axis of the piezoelectric phases, which also corresponds to the [111] axis of the magnetostrictive one, the shift of the resonant magnetic field is given by:

$$\delta H_E = \frac{3\lambda_{111}{}^{m}T_3}{M_0} = AE_3 \quad (15)$$

where M_0 is the saturation magnetization of the magnetostrictive layer, and the ME constant is defined by:

$$A = \frac{3\lambda_{111}}{M_0}\frac{\left(\frac{2^{p}c_{13}e_{31}}{^{p}c_{11}+^{p}c_{12}} - e_{33}\right)}{\left[1+\frac{^{m}v}{^{p}v}\left(\frac{1}{3^{m}c_{44}}+\frac{1}{3\left(^{m}c_{11}+2^{m}c_{12}\right)}\right)\left(^{p}c_{33}-2\frac{^{p}c_{13}^2}{\left(^{p}c_{11}+^{p}c_{12}\right)}\right)\right]} \quad (16)$$

From these equations, it is possible to estimate the shift of the resonant field for a bilayer magnetostrictive–piezoelectric composite. The theoretical values for the ME constant $A = \delta H_E/E_3$ were determined for composites of both nickel ferrite (NFO)–PZT and yttrium iron garnet (YIG)–PZT. For these calculations, the following materials parameters of two component phases were used:

YIG-PZT: $^{p}c_{11}=12.6\cdot10^{10}$ N/m^2; $^{p}c_{12}=7.95\cdot10^{10}$ N/m^2; $^{p}c_{13}=8.4\cdot10^{10}$ N/m^2; $^{p}c_{33}=11.7\cdot10^{10}$ N/m^2; e_{31}=-6.5 Sim/m^2; e_{33}=23.3 Sim/m^2; $\lambda_{111}=-2.4\cdot10^{-6}$; $4\pi M_0$=1750 Gs.

$NiFe_2O_4$: $^{m}c_{11}=21.99\cdot10^{10}$ N/m^2; $^{m}c_{12}=10.94\cdot10^{10}$ N/m^2; $^{m}c_{44}=8.12\cdot10^{10}$ N/m^2; $\lambda_{111}=-21.6\cdot10^{-6}$; $4\pi M_0$=3200 Gs.

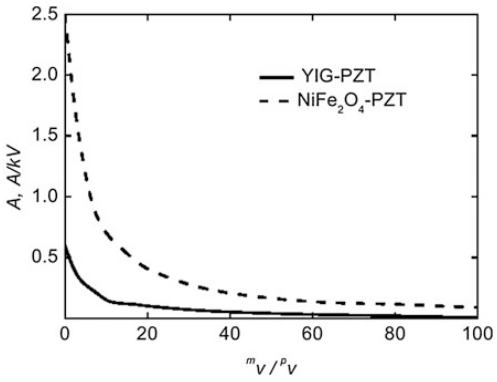

Figure 7. *Dependence of magnetoelectric constant A on volume fraction of magnetostrictive and piezoelectric phases$^{m}v/^{p}v$. The results are for bilayer composites of nickel ferrite–PZT and YIG–PZT.*

The values for the calculated resonance line shift (see Figure 7) are in good agreement with prior experimental data: theoretical line shift is 0.45 Oe-cm/kV, which is comparable to the measured one of 0.2–0.56 Oe-cm/kV depending on relative volume fraction of magnetostrictive and piezoelectric phases. Thus, we can see that it is necessary to use a piezoelectric component with large piezoelectric coefficients, and a magnetostrictive one with small saturation magnetization and high magnetostriction.

The results of ME interaction measurements in the microwave range in a two-layer structure based on YIG and PMN-PT single crystals are in Figure 8.

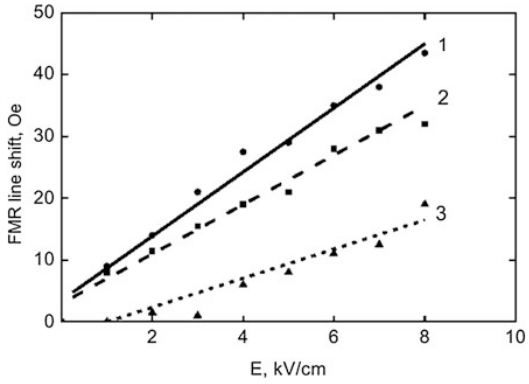

Figure 8. *The results of ME interaction measurements for a two-layer structure.*

Magnetoelectric effect in two-layer structures YIG (111) on GGG and PMN–PT (100) at frequency 9.3 GHz. Static fields E and H are parallel to an axis YIG [111] and perpendicular to sample plane. Shift of resonant magnetic field is shown as function E for different thickness of YIG film: 1—4.9 μm, 2—58 μm, 3—110μm.

The results of measurements of ME interaction in the microwave range in a two-layer structure based on YIG and PMN-PT single crystals are in Figure 9.

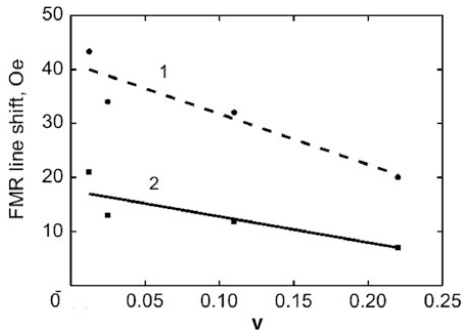

Figure 9. *Measured shift of resonant magnetic field in electric field E = 8 kV/sm as function of volume fractions of YIG and PMN–PT: 1 - H//[111], 2 - H//[011].*

The microwave ME effect depends near linearly on the relative volume fraction and much more than a width of FMR line (1-3 Oe). The shift in the resonant magnetic field induced by an external electric field can be seen to decrease with increasing volume fraction of YIG.

3.3. Magnetoelectric Effect in the MAR Range

A theoretical model predicts very strong ME interactions at

magnetoacoustic resonance (MAR) in single-crystal ferrite-piezoelectric bilayer. In such bilayers, the ME interactions are mediated by mechanical strain. The theory predicts efficient transfer of energy between phonons, spin waves, and electric and magnetic fields at MAR. Ultrahigh ME coefficients, on the order of 80–480 V/cm Oe at 5–10 GHz, are expected for nickel ferrite-PZT and yttrium-iron garnet-PZT bilayers. Effects of exchange interactions on magnetoacoustic resonance are taken into account.

ME effects in single-crystal ferrite-piezoelectric structures can be described by:

a) Equation of magnetization motion
b) Equation of ferrite medium motion
c) Equation of piezoelectric medium motion
d) Hooke's law for piezoelectric phase
e) Boundary conditions for displacement, stress, electric and magnetic fields.

Here we considered the bilayer composite as in Figure 10 with ferrite and piezoelectric single crystal layers. The ferrite layer is supposed to be in a saturated single domain state [24-29]. Bias field is assumed to be applied perpendicular to the sample plane. This state has two important advantages. First, when domains are absent, acoustic losses are minimum. Second, the single-domain state under FMR provides the conditions necessary for achieving a large effective susceptibility.

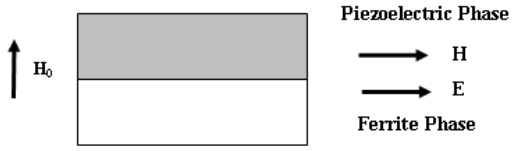

Figure 10. *Two-layer structure on the basis of single crystal phases.*

Direct magnetoelectric effect

The free energy density of a single crystal ferrite phase can be given as:

$$^{m}W = W_H + W_{an} + W_{ma} + W_{ac}; \quad (17)$$

where W_H=MH is Zeeman's energy, $W_{an}=K_1/M^4(M_1^2M_2^2+M_2^2M_3^2+M_3^2M_1^2)$ is cubic anisotropy energy, K_1 is a constant of the cubic anisotropy, $W_{ma}=B_1/M^2(M_1^{2m}S_1+M_2^{2m}S_2+M_3^{2m}S_3)+B_2/M^2(M_1M_2{}^{m}S_6+M_2M_3{}^{m}S_4+M_1M_3{}^{m}S_5)$ is the magnetoelastic energy, B_1 and B_2 are magnetoelastic constants, and $W_{ac}=½^{m}c_{11}(^{m}S_1^2+^{m}S_2^2+^{m}S_3^2)+½^{m}c_{44}(^{m}S_4^2+^{m}S_5^2+^{m}S_6^2)+^{m}c_{12}(^{m}S_1{}^{m}S_2+^{m}S_2{}^{m}S_3+^{m}S_1{}^{m}S_3$ is the elastic energy. In Eq. 17, it is supposed that the material is uniformly magnetized. On the basis of a generalized Hooke's law, we can write the stresses of the piezoelectric component phase as:

$$^{p}T_4 = {}^{p}c_{44}\,{}^{p}S_4 - e_{p15}\,{}^{p}E_2,$$
$$^{p}T_5 = {}^{p}c_{44}\,{}^{p}S_5 - e_{p15}\,{}^{p}E_1; \quad (18)$$

where e_{p15} is a shear piezoelectric coefficient. The equations of motion for the ferrite and piezoelectric phases are then

$$\partial^2({}^{m}u_1)/\partial t^2=\partial^2({}^{m}W)/(\partial x\partial {}^{m}S_1)+\partial^2({}^{m}W)/(\partial y\partial {}^{m}S_6)+\partial^2({}^{m}W)/(\partial z\partial {}^{m}S_5)$$
$$\partial^2({}^{p}u_1)/\partial t^2=\partial({}^{m}T_1)/\partial x+\partial({}^{m}T_1)/\partial y+\partial({}^{m}T_1)/\partial z, \quad (19)$$
$$\partial^2({}^{p}u_2)/\partial t^2=\partial({}^{m}T_2)/\partial x+\partial({}^{m}T_2)/\partial y+\partial({}^{m}T_2)/\partial z.$$

The equation of motion of the magnetization vector is given by:

$$\partial M/\partial t=-\gamma[M,H_{eff}], \quad (20)$$

Where $H_{eff}=-\partial({}^{m}W)/\partial M$.

To simply calculations, we assume waves with the circular polarization. Then we take into account the boundary conditions at the interface between layers and at the top/bottom planes of the composite, and use the open electric circuit condition.

An expression for the ME voltage coefficient is given by:

$$|E^+/H^+|=\gamma B_2{}^{p}c_{44}k_p{}^{p}e_{15}[1-\cos(k_p{}^{p}L)]^2/(\omega-\gamma H_0+4\pi\gamma M_0)\times[-½{}^{p}c_{44}{}^{p}\varepsilon_{33}k_p{}^{p}L\sin(2k_p{}^{p}L)({}^{p}c_{44}k_p+{}^{m}c_{44}k_m)+(\cos(k_p{}^{p}L)-1)\times{}^{p}e_{15}{}^2[(\cos(k_p{}^{p}L)({}^{m}c_{44}k_m+2\,{}^{p}c_{44}k_p)+{}^{m}c_{44}k_m]]\}, \quad (21)$$

where:

$$k_m=\omega\sqrt{\frac{{}^{m}\rho}{{}^{m}c_{44}}},\quad k_p=\omega\sqrt{\frac{{}^{p}\rho}{{}^{p}c_{44}}}$$

In Figure 11 and Figure 12 presented dependences of the ME voltage coefficient for a bilayer composite of single crystal YIG and PMN–PT.

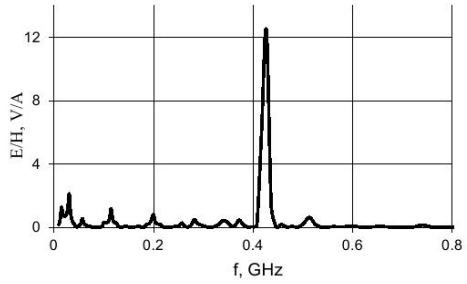

Figure 11. *Frequency dependence of ME voltage coefficient for L1=L2=0.05 mm, H_0=1.9 κOe.*

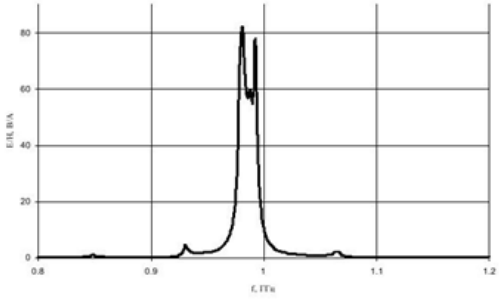

Figure 12. *Frequency dependence of ME voltage coefficient for L1=L2=0.01 mm, H_0=2.1 κOe.*

Calculations were performed by introducing a complex frequency to account for magnetoacoustic loss. The real component of the frequency was taken as $\omega_r=10^7$ rad/s.

For frequencies less than that of the homogeneous magnetization precession, the microwave ME voltage coefficient has a maximum when driven by an electric field in the EMR frequency range. Essential to this increase in the microwave ME voltage coefficient is that the EMR frequency of the electric be equal to that for a uniform magnetization precession in the ferrite phase. Even after including magnetoacoustic loss factors (as mentioned above), the microwave ME coefficient can reach giant values of up to 82 V/(cmOe).

Effects of Exchange Interactions on Magneto-Acoustic Resonance

It is well known that the influence of exchange interactions on magnetoelastic waves is stronger with frequency [24]. The exchange interaction determines the strength of the spin wave stiffness parameter and the frequency of the magnetoelastic modes.

The developed theory is applied to a YIG-PZT bilayer. The thicknesses of PZT and YIG layers are assumed to be 100 nm and 195 nm, respectively, so that the EMR thickness mode in PZT will have the same frequency as for FMR in YIG. Figure 13 shows the variation in α_E with f. The results are for bias fields H_0=1140 Oe for coincidence of FMR and fundamental EMR, and H_0=2850 Oe for the coincidence of FMR and higher harmonics of EMR. Consider the results for a bias field of 1140 Oe. A symmetric profile with a peak α_E of 65 V/cmOe is seen when the exchange parameter H_a=0. When the effect of exchange is considered, one notices a sharpening of the resonance profile with a 30% increase in ME coeffcient and a down shift in the resonance frequency. One obtains the "exchange amplification" of ME effect. The appearance of a high frequency shoulder is indicative of flow of RF energy to magnetoacoustic modes. Similar effects are expected for a frequency of about 10 GHz when the bias field is increased to 2850 Oe. When exchange interaction is considered, Figure 13 reveals a 60% increase in peak α_E and a broad shoulder due to magnetoacoustic excitations.

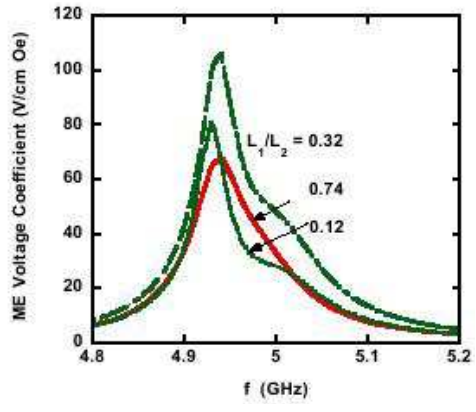

Figure 13. *The ME voltage coefficient α_E vs. frequency profile for a bilayer of lead zirconate titanate (PZT) of thickness 100 nm and yttrium iron garnet (YIG) of thickness 195 nm. Estimates are for magnetic exchange b=0 and b≠0 and dc magnetic fields of 1140 Oe and 2850 Oe.*

The discussed theory and estimates for YIG-PZT bilayers will be a roadmap for experiments on magnetoacoustic resonance and investigations on the effects of magnetic exchange interactions. Such bilayers and ME phenomenon are potentially useful for devices such as resonators or phase shifters based on magnetoacoustic waves.

4. Nomogram Method

Nomographs method can be used [30] when rough estimates are relevant and helpful. To plot the ME parameters versus initial material parameters and component volume fractions, we modelled the magnetic field induced ME effect for several operational modes and laminate composites of most importance to application in electronic devices. In particular, we considered longitudinal and bending modes, laminates of homogeneous and compositionally stepped piezoelectrics and magnetostrictive materials [33]. Nomographs can be used for a quick test of ME composites for applications where an approximate answer is appropriate and useful.

Low-frequency magnetoelectric coupling

As an example (see Figure 14), estimates are obtained for transverse fields' orientation (in-plane ac and dc magnetic fields and out-of-plane ac electric field and poling direction). For symmetric trilayer structures the expression for transverse ME voltage coefficient takes on the form:

$$\alpha_{E,31}=\frac{V(1-V)x}{\varepsilon_0[{}^{m}s_{11}V+{}^{p}s_{11}(1-V)]} \tag{22}$$

Where $x={}^{m}q_{11}{}^{p}d_{31}\varepsilon 0/{}^{p}\varepsilon_{33}$, ${}^{p}s_{11}$, ${}^{m}s_{11}$, ${}^{p}d_{31}$ and ${}^{m}q_{11}$ are compliance, and piezoelectric and piezomagnetic coupling coefficients for piezoelectric and piezomagnetic layers, respectively, ${}^{p}\varepsilon_{33}$ is the permittivity of piezoelectric layer, V is volume fraction of piezoelectric and magnetic phases.

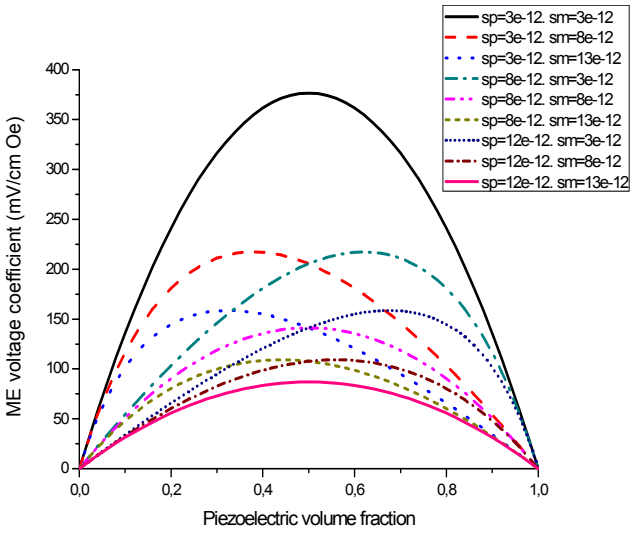

Figure 14. *Piezoelectric volume fraction dependence of transverse ME voltage coellicient for simmetric layered structure of magnetoctrictive and piezoelectric components with different complienceces for $x=0.5\cdot10^{-22}$ (in SI units).*

Magnetoelectric coupling at axial mode

Small-amplitude axial oscillations of the layered structures formed by magnetostrictive and piezoelectric phases:

$$\frac{\alpha_E}{Q_a} = \frac{8}{\pi^2} \frac{V(1-V)^m q_{11}{}^p d_{31} \Big/ {}^p\varepsilon_{33}}{\left[V^m s_{11} + (1-V)^p s_{11}\right]} \quad (23)$$

where Q_a is the quality factor for the EMR resonance.

The results of calculations are presented in Figure 15.

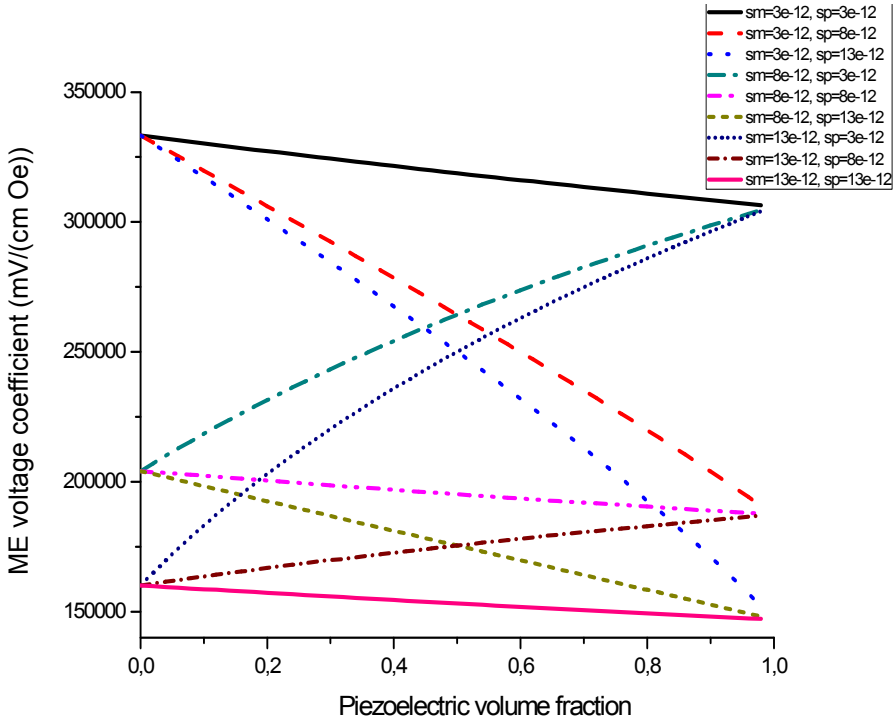

Figure 15. *EMR frequency versus piezoelectric volume fraction for longitudinal mode of 10 mm long magnetostrictive-piezoelectric layered structure.*

Magnetoelectric coupling in FMR region

As an example, we consider a specific case of magnetic field *H* along [111] axis (Figure 16 and Figure 17).

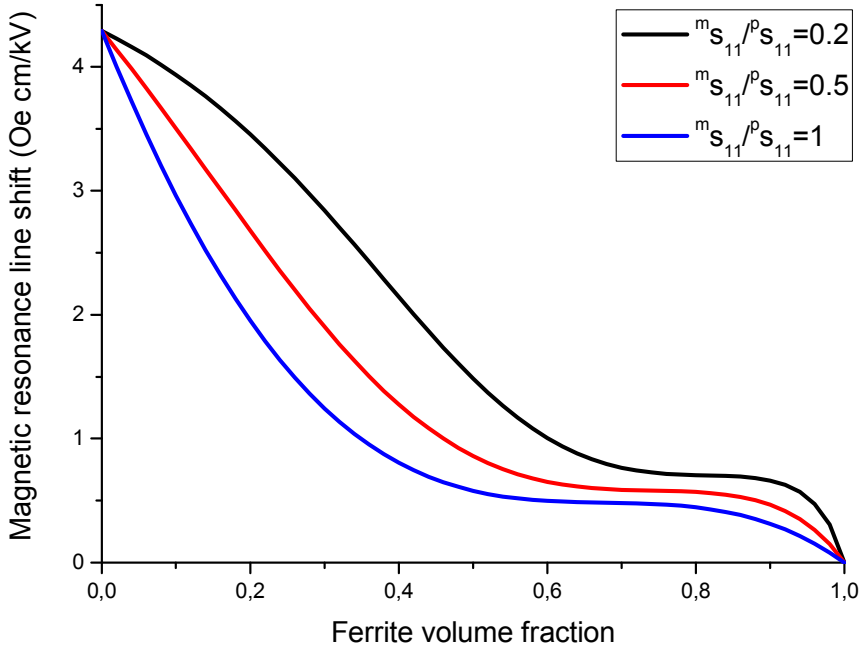

Figure 16. *Ferrite volume fraction dependence of magnetic resonance line shift at E=1 kV/cm for ferrite-piezoelectric bilayer for* $\lambda_{111}/M_s=0.16\cdot10^{-8}$ Oe^{-1}.

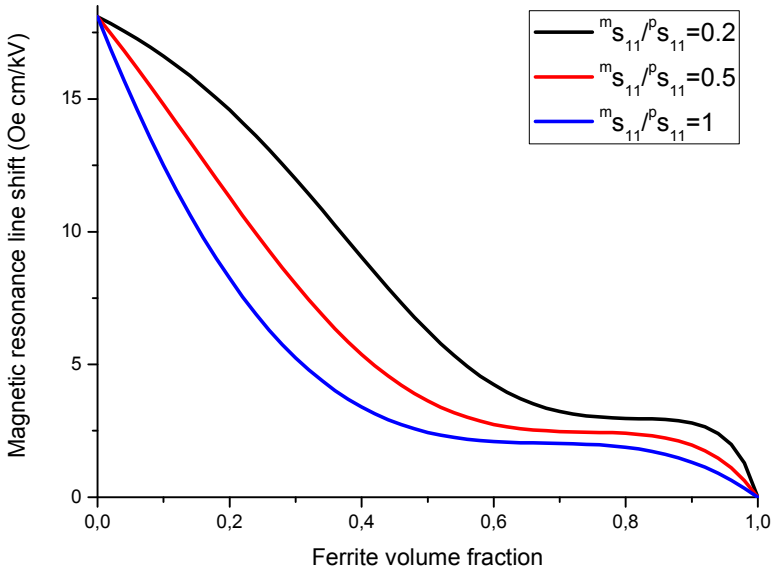

Figure 17. *Ferrite volume fraction dependence of magnetic resonance line shift at E=1 kV/cm for ferrite-piezoelectric bilayer for $\lambda_{111}/M_s=0.68\cdot10^{-8}$ Oe^{-1}.*

To obtain the estimates of ME coefficients from nomographs referred to above, one should use the material parameters of composite components. The relevant parameters of several materials that are most often used in ME structures are given in Table 1.

From the results for FMR region, we can conclude to obtain an optimum ME effect in FMR region: (i) that the volume fraction of the piezoelectric phase should be high; (ii) that it is necessary to use a piezoelectric component phase with a large piezoelectric coefficient; and (iii) that it is necessary to use a magnetostrictive component phase with a small saturation magnetization and a high magnetostriction [30].

Table 1. *The material parameters of composite components.*

Material	**s_{11} (10^{-12} m^2/N)**	**q_{33} (10^{-12} m/A)**	**d_{31} (10^{-12} m/V)**	**d_{33} (10^{-12} m/V)**	**λ_{100} (10^{-6})**	**$\varepsilon_{33}/\varepsilon_0$**
PZT	15.3	-	-175	400	-	1750
BTO	7.3	-	-78		-	1345
PMN-PT	23	-	-600	1500		5000
Langasite	8.8	-	$d_{14}=-3.65\cdot10^{-12}$ m/V	$d_{11}=6.3\cdot10^{-12}$ m/V		50
Langatite	9.8	-	$d_{14}=-2.81\cdot10^{-12}$ m/V	$d_{11}=7.4\cdot10^{-12}$ m/V		77
Quartz	12.8	-	$d_{14}=-0.67\cdot10^{-12}$ m/V	$d_{11}=2.3\cdot10^{-12}$ m/V		4.68
YIG	6.5		-	-	1.4	10
NFO	6.5	-680	-	-	23	10
LFO	35				46	10
Ni	20	-4140				
Terfenol-D	33.3	15707	-	-		
Metglas	10	14000	-	-		

Nomographs can be used for a quick test of ME composites and useful for creation of new ME composites with enhanced ME couplings that would enable them for application in functional electronics devices.

5. Application of Magnetoelectric Composites

Composite materials, on the other hand, provide an alternative strategy which makes use of indirect coupling via mechanical strain between the materials of two different phases: ferroelectric and ferromagnetic (or antiferromagnetic or ferrimagnetic such as ferrites). Mechanical deformation of the magnetostrictive phase results in polarization in the piezoelectric phase. ME effect in composites may be more than several orders of magnitude higher than that in single phase materials, the latter forming actually the basis for much hyped multiferroics. Such composites can be implemented in the form of "multilayers" consisting of alternating layers of the ferroelectric phase and the ferro- or ferri-magnetic phase. Bilayers and multilayers of composites are especially promising due to their low leakage current and superior poling properties. In multilayers, however, the magnetoelectric coupling effect is weakened due to the clamping effect of the substrate, unless the multilayers are fabricated as free standing membranes.

In the discussion of linear and higher order magnetoelectrical coupling, we have so far ignored the effects of strain. However, inclusion of strain arising from piezomagnetism and magnetostriction would introduce cross terms that are proportional to strain and have linear and/or quadratic dependence on magnetic field H. Similarly,

additional terms would arise from piezoelectricity and electrostriction, having dependences on electric field E. Even mixed terms involving strain, H, and E would appear. The effects of strain are significant and in some cases may even dominate which actually desired in laminated two-layer composites. Most ferromagnetic materials exhibit magnetostriction, which describes a change in strain as a quadratic function of the applied magnetic field. This change in the strain may induce polarization in the ferroelectric phase, which is in contact with the ferromagnetic/antiferromagentic/ferromagnetic phase (ideally in atomic registry), through the piezoelectric effect.

For the two-phase systems, the physical properties are determined by the interaction between the constituents as well as by their individual properties. Some effects, which are already present in the constituents may be averaged or enhanced for the overall system. However, the ME effect is among the novel effects that arises from the product properties originating through the interaction between the two phases. The ME effect can be achieved by coupling a piezoelectric (or electrostrictive) material and a piezomagnetic (or magnetostrictive) material via a good mechanical contact. Such a two-phase system may be achieved in the form of composites, laminates, or epitaxial layers. Miniaturization of microwave devices is one of the fundamental requirements in communication systems. Therefore, small-size and high performance devices are always necessary to reduce cost and enhance system performance. Today there is the diversified production engineering of forming of electric circuits with the small losses, manifesting frequency-dependent properties. It is possible to following constructive alternatives.

Layered structure based on the magnetostrictive and piezoelectric materials are perspective for design of new microwave devices. The given materials contain magnetostrictive and piezoelectric components and possess magnetoelectric interaction that will allow creating essentially new devices on their basis [9-15].

Low frequency device

As an example of low frequency device we presented magnetoelectric current sensor with higher sensitivity and higher radiation stability of sensitive element which significantly increases application possibilities of such sensor [31, 32]. In Figure 18 a schematic diagram of sensor is represented.

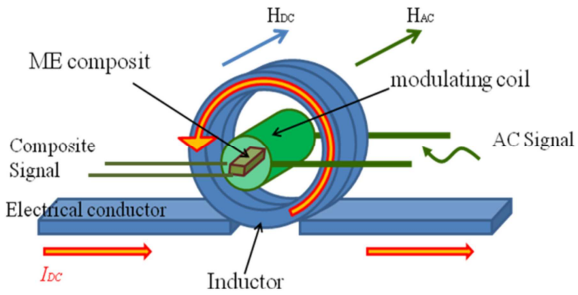

Figure 18. *Schematic diagram of sensor.*

Figure 19. Shows the photography of sensor sample.

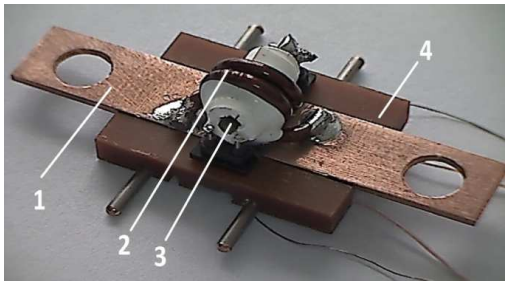

Figure 19. *Photography of sensor sample. 1 is conductor, 2 is coil, 3 is ME composite, 4 is case.*

Characteristics of ME sensor: power supply 5±0,5 V; measuring range current, 0...5A; non-linearity less than 1%; sensitivity 0,7 V/A; consumption current 2,5 mA; dimensions 30x20x10mm.

Figure 20 shows an experimental results for ME current sensor.

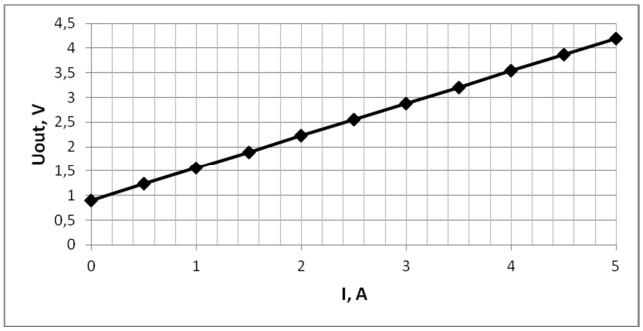

Figure 20. *An experimental results for ME current sensor.*

The main directions of application are information and telecommunication systems, transport and space systems.

Microwave and mm-wave components and devices

For the estimation of device characteristics, we consider the transmission lines and the resonator (Figure 21) as a single system that is described by a coupling coefficient.

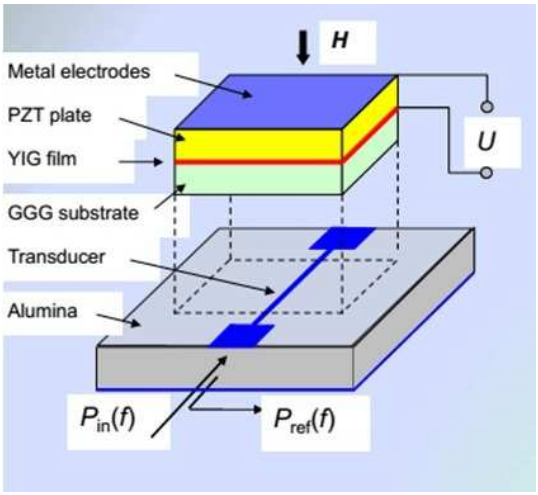

Figure 21. *Schematic diagram of ME resonator and transmission line.*

We follow a two stage procedure for the device design: first we obtain the coefficients of reflection, transmission and

absorption for the case when an ME resonator is considered as an irregularity in the transmission line. Then we take into account the number of resonators to estimate the coupling coefficient. As model of the multi-resonators devices the single-resonators devices joined by a piece of transmission line of nonresonance length, carrying out a role of connection device between parts is accepted. Thus, the transfer ratio of the cascade-type devices can be obtained from a transfer ratio for the single-resonator devices.

As an example of one resonator system we are proposed magnetoelectric attenuator (Figure 22) with dual tunability possibilities of control and higher radiation stability of ME element which significantly increases application possibilities of such devices.

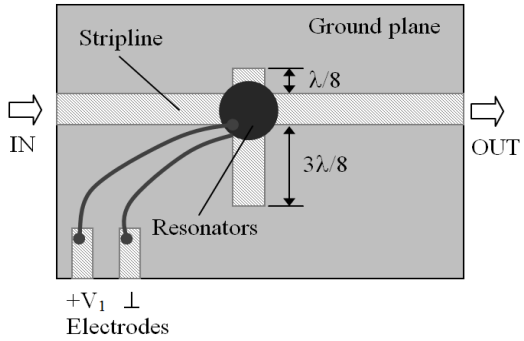

Figure 22. *Schematic diagram of ME attenuator. Frequency range 4,0-18,0 GHz; Attenuation 0-25 dB; Phase shift ±45 degree; Power management ±100 V; Dimensions 30x20x10mm.*

Magnetoelectric microwave attenuator is a resonant type of devices which are controlled by an electric or magnetic field. The basis of the device is a microstrip transmission line and a ME resonator based on ferrite-piezoelectric components.

Microwave measurements were carried out using a vector network analyzer. A standard calibration procedure was performed before measurements. A microwave input signal at 7.25 GHz and power P_{in}=0.1 mW was applied to the microstrip transducer. Low input power was chosen to prevent heating of the sample due to power absorption at FMR. Profiles of $S_{21}(f)$=10log[($P_{out}(f)/P_{in}(f)$] vs. f, for an in-plane magnetic field H_0=1.91 kOe are shown in Figure 23.

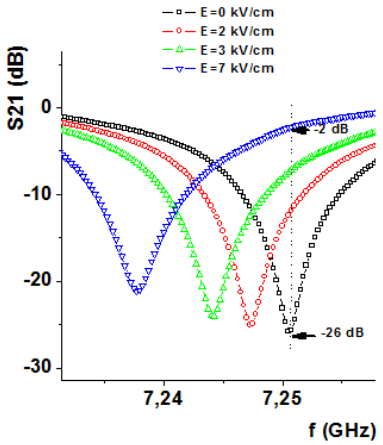

Figure 23. *Profiles of $S_{21}(f)$ for attenuator.*

These data were obtained by setting the bias field $H=H_0$ and by increasing E from 0 to 7 kV/cm. With increasing E, one observes a sharp decreasing in attenuation up to 5 kV/cm and then it levels off at 2 dB. The power absorbed by the ME element is given by:

$$P(H) = P_0 \exp[-\gamma \frac{(H-H_0)^2}{2\sigma^2}] \quad (24)$$

where γ is the gyromagnetic ratio, H is the effective bias magnetic field, P_0 is absorption at the resonance field H_0, and σ is a parameter determined from the width of resonance line. The electric field leads to a frequency shift δf of the resonance profiles by $\delta f=\gamma(H-H_0)=AE$. Insertion loss of ME element can be expressed as:

$$L = 20\log[1-(1-|s_{21}(H_0)|^2)]\exp(-A^2E^2/(2\sigma^2)) \quad (25)$$

Here $S_{21}(H_0)$ is the S-parameter at resonance and for E=0. For the estimation of dependence of insertion loss L vs electric field E, we used measured values of A=2 MHz·cm/kV and $S_{21}(H_0)$=0.22 and choose σ=6 MHz.

In Figure 24 the attenuation parameter as a function of electric field E is presented.

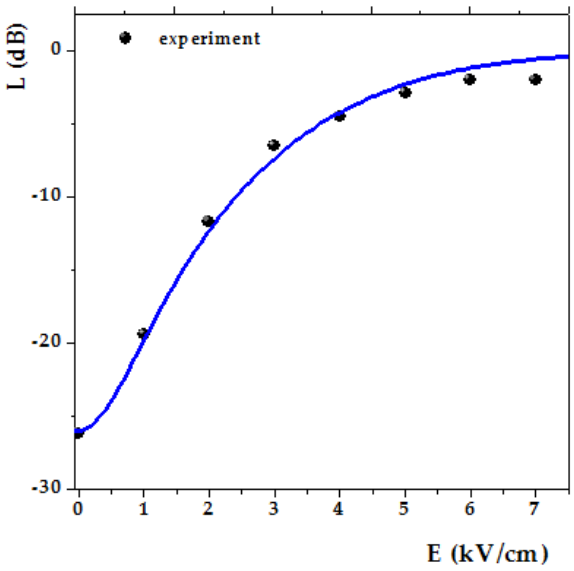

Figure 24. *The attenuation as a function of electric field E.*

Ferrite-piezoelectric heterostructures are ideal for studies on wide-band magnetoelectric interactions between the magnetic and electric subsystems that are mediated by mechanical forces. Such structures show a variety of magneto-electric phenomena including microwave ME effects. The phenomenon can be used for creation electrical tuning magnetoelectrical microwave resonators and devices on their basis. The specific focus is on ME effects when electromagnetic modes close to FMR are excited in the ferrite. In the presence of an electric field, the piezoelectric deformation in the bilayer will manifest as an internal magnetic field in the ferrite. Tunability of the ME devices

characteristics in the chosen working range can be executed by application of an electric field. This electric tuning is relatively fast and is not power-consuming.

6. Conclusions

Modeling of ME composites at low frequencies and in the field of electromechanical, ferromagnetic and magnetoacoustic resonances has shown that they can be effectively used to design various electronic devices in a wide frequency range [34].

For such characteristics as speed; power, in control circuits; electromagnetic compatibility; radiation resistance, ME devices are close to ferroelectric devices with their advantages due to ceramic technology and a low-inertia control system for the electric field. At the same time, ME devices potentially have better thermal stability, the possibility of interaction with both electric and magnetic components of the electromagnetic field. Examples of application of ME composites: magnetic field sensors, current sensors, microwave phase shifters, filters, attenuators, isolators, etc.

Problems that need to be solved: develop glue less technology for the production of multilayer ME structures, increase the sensitivity and reduce the size of ME devices, reduce the values of the control electric and magnetic fields, research and develop microwave ME devices based on slot and coplanar strip lines, research and develop active ME devices.

Acknowledgements

This work was supported by the Russian Foundation for Basic Research (grant 19-57-53001).

References

[1] *Magnetoelectricity in Composites.* Eds. M. Bichurin, D. Viehland. Pan Stanford Publishing, Singapore, 2012, 273p.

[2] M. Bichurin, V. Petrov, *Modeling of Magnetoelectric Effects in Composites*. Springer Series in Materials Science, 201, 2013, 108p.

[3] Ce-Wen Nan, M. I. Bichurin, Shuxiang Dong, D. Viehland, G. Srinivasan, J. Appl. Phys 103, 031101 (2008).

[4] M. I. Bichurin, V. M. Petrov, G. Srinivasan, Ferroelectrics 280, 165 (2002).

[5] M. I. Bichurin., V. M. Petrov, G. Srinivasan, J. Appl. Phys. 92, 7681 (2002).

[6] M. I. Bichurin, V. M. Petrov, G. Srinivasan, Phys. Rev. B. 68, 054402 (2003).

[7] M. I. Bichurin, V. M. Petrov, G Srinivasan, J. of Magnetism and Magnetic Materials 321, 846 (2009).

[8] V. Gheevarughese, V. M. Laletsin, V. M. Petrov, G. Srinivasan, N. A. Fedotov, J. of materials research 22, 2130 (2007).

[9] M. I. Bichurin, V. M. Petrov, Technical Physics 58, 2277 (1988).

[10] M. I. Bichurin, I. A. Kornev, V. M. Petrov, A. S. Tatarenko, Yu. V. Kiliba, and G. Srinivasan, Phys. Rev. B. 64, 094409 (2001).

[11] S. Shastry, G. Srinivasan, M. I. Bichurin, V. M. Petrov, A. S. Tatarenko, Phys. Rev. B. 70, 064416 (2004).

[12] M. I. Bichurin, V. M. Petrov, O. V. Ryabkov, S. V. Averkin, and G. Srinivasan, Phys. Rev. B 72, 060408 (R) (2005).

[13] M. I. Bichurin, V. M. Petrov, R. V. Petrov, G. N. Kapralov, F. I. Bukashev, A. Yu. Smirnov, A. S. Tatarenko, Ferroelectrics 280, 213 (2002).

[14] A. S. Tatarenko, M. I. Bichurin, Advances in Condensed Matter Physics 10, 2012 (2012).

[15] A. S. Tatarenko, M. I. Bichurin, American J. Cond. Matt. Phys. 2 (5), 135 (2012).

[16] M. I. Bichurin, V. M. Petrov, S. V. Averkin, E. Liverts, Journal of applied physics 107, 053904 (2010).

[17] M. I. Bichurin, V. M. Petrov, R. V. Petrov, Journal of Magnetism and Magnetic Materials 324, 3548 (2012).

[18] M. I. Bichurin, V. M. Petrov, R. V. Petrov, S. Priya, Solid State Phenomena 189, 129 (2012).

[19] M. I. Bichurin, I. A. Kornev, V. M. Petrov, and I. V. Lisnevskaya. Ferroelectrics, 204, 289 (1997).

[20] N. Zhang, V. M. Petrov, T. Johnson, S. K. Mandal, G. Srinivasan, Journal of Applied Physics 106, 126101 (2009).

[21] M. I. Bichurin, Yu. N. Venevtsev, O. S. Didkovskaya, V. M. Petrov, N. N. Fomich, "Magnetoelectric materials: technology features and application perspectives". In: *Magnetoelectric Substances*, Nauka, Moscow, Russia, p. 118-132 (1990) (in Russian).

[22] G. Srinivasan., *Annu. Rev. Mater. Res. 40*, 153 (2010).

[23] M. I. Bichurin, V. M. Petrov, R. V. Petrov, F. I. Bukashev, A. Y. Smirnov. Ferroelectrics 280, 203 (2002).

[24] O. V. Ryabkov, V. M. Petrov, M. I. Bichurin, G. Srinivasan, Technical Physics Letters 32, 1021 (2006).

[25] O. V. Ryabkov, S. V. Averkin, M. I. Bichurin, V. M. Petrov, G. Srinivasan, Journal of materials research 22, 2174 (2007).

[26] M. I. Bichurin, V. M. Petrov, S. V. Averkin, A. V. Filippov, E. Liverts, S. Mandal, Journal of Physics D: Applied Physics 42, 215001 (2009).

[27] V. M. Petrov, V. V. Zibtsev, G. Srinivasan, The European Physical Journal B 71, 367 (2009).

[28] V. M. Petrov, G. Srinivasan, O. V. Ryabkov, S. V. Averkin, M. I. Bichurin, Solid State Communications 144, 50 (2007).

[29] M. I. Bichurin, Ferroelectrics 161, 53 (1994).

[30] M. Bichurin, V. Petrov, R. Petrov, A. Tatarenko, V. Leontiev, K. Lavrentieva, JMMM, 412, 1 (2016).

[31] M. I. Bichurin, V. M. Petrov, R. V. Petrov, A. S. Tatarenko. Magnetoelectric magnetometers. In *High Sensitivity Magnetometers*. Eds. A. Grosz et al. © Springer International Publishing Switzerland 2016; pp 127-166.

[32] M. Bichurin, R. Petrov, V. Leontiev, G. Semenov, O. Sokolov. Sensors, 17, 1271 (2017).

[33] M. I. Bichurin, V. M. Petrov, G. A. Semenov, "Magnetoelectric material for components of radioelectronic devices," Patent № RU 2363074 C1 (submitted 11.03.2008, published 27.07.2009).

[34] *Magnetoelectric Composites* Mirza I. Bichurin, Vladimir M. Petrov, Roman V. Petrov, and Alexander S. Tatarenko Pan Stanford Publishing Pte. Ltd. Singapore, 2019, 280p.